Opioid Receptors Inhibit the Spinal AMPA Receptor Ca^{2+} Permeability that Mediates Latent Pain Sensitization

Bradley K. Taylor[a,b,*], **Ghanshyam P. Sinha**[a,b], **Renee R. Donahue**[b], **Carolyn M. Grachen**[a,b], **Jose A. Morón**[c], and **Suzanne Doolen**[a,b,*]

[a]Department of Anesthesiology, Pittsburgh Center for Pain Research, University of Pittsburgh School of Medicine, 200 Lothrop St. Pittsburgh, PA 15213, USA

[b]Department of Physiology, University of Kentucky School of Medicine, 800 Rose St. Lexington, KY 40536-0298, USA

[c]Department of Anesthesiology, Washington University Pain Center, Washington University School of Medicine, 600 South Euclid, St Louis, MO 63110, USA

Abstract

Acute inflammation induces sensitization of nociceptive neurons and triggers the accumulation of calcium permeable (CP) α-amino-3-hydroxy-5-methyl-4-isoxazole propionic acid receptors (AMPARs) in the dorsal horn of the spinal cord. This coincides with behavioral signs of acute inflammatory pain, but whether CP-AMPARs contribute to chronic pain remains unclear. To evaluate this question, we first constructed current-voltage (I-V) curves of C-fiber stimulus-evoked, AMPAR-mediated EPSCs in lamina II to test for inward rectification, a key characteristic of CP-AMPARs. We found that the intraplantar injection of complete Freund's adjuvant (CFA) induced an inward rectification at 3 d that persisted to 21 d after injury. Furthermore, the CP-AMPAR antagonist IEM-1460 (50 μM) inhibited AMPAR-evoked Ca^{2+} transients 21d after injury but had no effect in uninflamed mice. We then used a model of long-lasting vulnerability for chronic pain that is determined by the balance between latent central sensitization (LCS) and mu opioid receptor constitutive activity (MOR$_{CA}$). When administered 21d after the intraplantar injection of CFA, intrathecal administration of the MOR$_{CA}$ inverse agonist naltrexone (NTX, 1 μg, *i.t.*) reinstated mechanical hypersensitivity, and superfusion of spinal cord slices with NTX (10 μM) increased the peak amplitude of AMPAR-evoked Ca^{2+} transients in lamina II neurons. The CP-AMPAR antagonist naspm (0–10 nmol, *i.t.*) inhibited these NTX-induced increases in mechanical hypersensitivity. NTX had no effect in uninflamed mice. Subsequent western blot analysis of the postsynaptic density membrane fraction from lumbar dorsal horn revealed that CFA increased GluA1 expression at 2 d and GluA4 expression at both 2 and 21 d post-injury, indicating that not just the GluA1 subunit, but also the GluA4 subunit, contributes to the expression of CP-AMPARs and synaptic strength during hyperalgesia. GluA2 expression increased at 21 d, an unexpected result that requires further study. We conclude that after tissue injury, dorsal horn AMPARs retain a Ca^{2+} permeability that underlies LCS. Because of their effectiveness in reducing

---

*Corresponding authors: Bradley K. Taylor and Suzanne Doolen, Ph.D. Department of Anesthesiology, University of Pittsburgh, 200 Lothrop St. Pittsburgh, PA 15213, BKT@pitt.edu.

Disclosures: The authors declare no competing financial accests.

naltrexone-induced reinstatement of hyperalgesia and potentiation of AMPAR-evoked Ca^{2+} signals, CP-AMPAR inhibitors are a promising class of agents for the treatment of chronic inflammatory pain.

Keywords

hyperalgesia; Ca^{2+} permeable AMPA receptor; chronic pain; inflammation; Ca^{2+} imaging; sensitization; dorsal horn; postsynaptic density

1. Introduction

Tissue injury and the resulting inflammation increases the responsiveness of spinal cord nociceptive neurons in the dorsal horn (DH) to normal or sub-threshold afferent input, termed central sensitization (CS). We and others have proposed an even longer-lasting form of CS that outlasts physical damage and inflammation, termed latent central sensitization (LCS) (Campillo et al., 2011; Corder et al., 2013; Taylor and Corder, 2014; Walwyn et al., 2016). LCS is kept within a months-long remission phase by mu opioid receptor constitutive activity (MOR_{CA}). For example, hindpaw injection of complete Freund's adjuvant (CFA) increased mechanical sensitivity *in vivo* and potentiated glutamate-evoked intracellular Ca^{2+} signals in lamina II neurons of spinal cord slices *in vitro*. Both of these responses resolved within 1–2 weeks, after which subsequent disruption of MOR_{CA} with an inverse agonist such as naltrexone (NTX) reinstated hypersensitivity not only in mice and rats, but also in humans (Campillo et al., 2011; Corder et al., 2013; Springborg et al., 2016; Walwyn et al., 2016). Because AMPARs contribute to the CS associated with acute pain (Cabanero et al., 2013; Chen et al., 2013; Katano et al., 2008; Park et al., 2009; Vikman et al., 2008; Voitenko et al., 2004), here we asked whether they also contribute to the LCS associated with chronic pain.

AMPARs are comprised of four subunits (GluA1–4) that assemble as tetramers (Keinanen et al., 1990). Under normal conditions, most AMPARs in the CNS, including those within laminae I–IV of the DH, are Ca^{2+}-impermeable due to the presence of one or more GluA2 subunits (Burnashev et al., 1992; Hollmann et al., 1991). The incorporation of GluA2-lacking, Ca^{2+}-permeable AMPARs (CP-AMPARs) increases soon after injury in animal models of inflammatory pain (Atianjoh et al., 2010; Choi et al., 2010; Galan et al., 2004; Katano et al., 2008; Larsson and Broman, 2008; Park et al., 2009; Park et al., 2008; Vikman et al., 2008; Voitenko et al., 2004; Wigerblad et al., 2017) neuropathic pain (Chen et al., 2013; Chen et al., 2016b) and opioid-induced hyperalgesia (Cabanero et al., 2013). Spinal CP-AMPARs appear to drive activity-dependent changes in synaptic processing of nociceptive inputs. For example, inflammation-induced potentiation and spatial spread of spinal calcium transients is lost in mice lacking CP-AMPARs (Luo et al., 2008).

Previous studies show that CP-AMPARs are regulated differently in excitatory and inhibitory neurons (Chen et al., 2016b; Kopach et al., 2015). For example, Chen et al. found that chronic constriction injury (CCI) produced a loss of synaptic CP-AMPARs on inhibitory (tonic firing) neurons but not on excitatory (delayed firing) neurons (Chen et al., 2016b). However, the above studies were limited, however, to early time points (days to a couple of

weeks after injury). To determine whether CP-AMPARs contribute to the more chronic phases of inflammatory pain, we used our CFA model of LCS / MOR$_{CA}$.

2. Materials and methods

Animals

Adult male C57Bl/6 mice (7–9 weeks old for behavioral and biochemical studies, 3 weeks old for Ca^{2+} imaging and electrophysiology studies) were purchased from Charles River Laboratories (Indianapolis, IN). Mice were housed 4 per cage in a temperature controlled (68–72° F) room on a 14:10 hour light/dark cycle (dark hours from 8PM-6AM) and given food and water *ad libitum*. All procedures were approved by the Institutional Animal Care and Use Committee at the University of Kentucky in accordance with the American Veterinary Medical Association guidelines.

Complete Freund's Adjuvant (CFA) model of inflammatory pain

Animals were allowed at least four days to habituate to the facility before the beginning of the study. Immediately following baseline assessment of mechanical thresholds, male C57Bl/6 mice, were lightly restrained and subcutaneously injected with CFA (5–10 μl, non-diluted) under the ventromedial surface of the left hindpaw. In electrophysiological and behavioral studies, sham mice were injected with an equal volume of saline to control for needle puncture and injectate volume.

Intrathecal drug administration

Unanesthetized mice were lightly restrained and a 30 G needle attached to a Hamilton microsyringe was inserted between the L5/L6 vertebrae. After intrathecal placement was confirmed by the presence of a reflexive tail flick as previously described (Fairbanks, 2003), 5 μl of NTX or saline and 5 ul of naspm or saline were injected together.

Tactile threshold

Mice were acclimated for 30 – 60 min in the testing environment within a rectangular plastic box (15×4×4 cm; 3 white opaque walls and 1 clear wall) on a raised metal mesh platform. Baseline testing was conducted prior to and after injury and at various time points after drug injection (as indicated by an arrow in the figures). To evaluate mechanical hypersensitivity (hyperalgesia) we used a logarithmically increasing set of 8 von Frey filaments (Stoelting, Illinois), ranging in gram force from 0.007 to 6.0 g. These were applied perpendicular to the ventral-medial plantar hindpaw surface with sufficient force to cause a slight bending of the filament. A positive response was characterized as a rapid withdrawal of the paw away from the stimulus fiber within 4–5 s. Using Dixon's up–down statistical method, modified by Chaplan et al. (Chaplan et al., 1994), the 50% withdrawal mechanical threshold score was calculated for each mouse and then averaged across the experimental groups.

Adult mouse spinal cord slices

Mice were anesthetized with 5% isoflurane and perfused transcardially over the course of approximately one minute with 10 ml of ice-cold sucrose-containing artificial cerebrospinal

fluid (sucrose-aCSF) that contained (in mM): NaCl 95, KCl 1.8, KH_2PO_4 1.2, $CaCl_2$ 0.5, $MgSO_4$ 7, $NaHCO_3$ 26, glucose 15, sucrose 50, kynurenic acid 1, oxygenated with 95% O_2, 5% CO_2; pH 7.4 (Doolen et al., 2012). The lumbar spinal cord was rapidly isolated by laminectomy from the cervical enlargement to the cauda equina, placed in oxygenated ice-cold sucrose-aCSF, cleaned of dura mater and ventral roots, cut in the transverse orientation across the lumbar enlargement, and glued with cyanoacrylate to an agar block (Fisher Scientific, Pittsburgh, PA) on the stage of a Campden 5000mz vibratome (Lafayette, IN). Lumbar segments L3-L4 were cut (300 μm ipsilateral sagittal slice with dorsal root attached for electrophysiology; 450 μm transverse slices for Ca^{2+} imaging) in ice-cold sucrose-aCSF using minimal forward speed (0.01 – 0.04 mm/s) and maximum vibration (50 Hz).

Calcium imaging

Slices were incubated for 30 min at room temperature with Fura-2 AM (10 mM) in oxygenated normal aCSF that contained pluronic acid (0.1%) and (in mM): NaCl 127, KCl 1.8, KH_2PO_4 1.2, $CaCl_2$ 2.4, $MgSO_4$ 1.3, $NaHCO_3$ 26, glucose 15, followed by a 20 min de-esterification period (Corder et al., 2013; Doolen et al., 2012). Slices were perfused at 1–2 ml/min with normal aCSF in a recording chamber (RC-25, Warner instruments, Hamden, CT) mounted on a Nikon FN-1 upright microscope with a 79000 ET FURA2 Hybrid filter set and a Photometrics CoolSNAP HQ_2 camera. Relative intracellular Ca^{2+} levels were determined by measuring the change in ratio of fluorescence emission at 510 nm in response to excitation at 340 and 380 nm. Paired images were collected at 1 frame/second. Relative intracellular Ca^{2+} levels were evaluated in single cells by creating a region of interest over each cell body (with preference given to profiles with high fluorescence at 380 nm) using Nikon Elements software, and then calculated as the peak magnitude of the   340/380 ratio. Regions of interest (ROIs) that did not respond to glutamate (~20%), and cells that displayed a large run-down in response to 1.0 mM glutamate (cells with more than a 40% decrease in glutamate-evoked Ca^{2+} transients from the beginning to the end of the recording session yielded inconsistent results, ~20%) were excluded. Slices were studied within 8 hours of dissection. At 20x magnification, we observed 8.4 ± 0.6 of glutamate-responsive fura-2-positive cells per field of view. Cells from 1–2 slices were averaged within each animal, and n was defined by number of animals.

Electrophysiology

Whole-cell patch-clamp recordings were collected with a Multiclamp 700B amplifier (Molecular Devices, Sunnyvale, CA, USA). Glass pipette patch electrodes were filled with a cesium-based solution containing (in mM): Cs-Glu 130, CsCl 10, HEPES 10, EGTA 11, $CaCl_2$ 1, Mg-ATP 2 and Na_4-GTP 0.2, pH 7.2 (~300 mOsm). 5 mM Qx314.Cl and 0.1 mM spermine tetrahydrochloride were added to the pipette solution. Pipette resistance ranged from 4 to 6 MΩ. Currents were filtered at 4–6 kHz through a four-pole low-pass Bessel filter and digitally sampled at 20 kHz (Digidata 1440A with pClamp 10.3 software; Molecular Devices).

Slices were perfused at 3 ml/min with normal aCSF in the recording chamber (RC-27, Warner instruments, Hamden, CT) mounted on an upright Olympus BX51W1 microscope and studied within 5 hours of dissection. All recordings were conducted at RT. With a glass

suction electrode, the attached dorsal root was exposed to electrical stimuli of increasing intensity (0.1 – 3 mA), 0.1 ms duration, and 0.02 Hz frequency to evoke C-fiber mediated EPSCs (Nakatsuka et al., 2000; Torsney and MacDermott, 2006). Monosynaptic EPSCs in laminae II neurons were selected with the following criteria: 1) constant response latency (i.e., response variability or "jitter" < 200 μs) even as the intensity of dorsal root stimulation (DRS) was increased; and 2) EPSC response failures at frequency stimulation   2 Hz (C-fiber stimulations fail to elicit consistent action potential responses above 2 Hz (Nakatsuka et al., 2000)). To pharmacologically isolate AMPAR-mediated EPSCs, recordings were performed in the presence of bicuculline (10 μM), CGP55845 (2 μM), strychnine (2 μM) and AP5 (50 μM). All AMPAR-mediated EPSCs were confirmed at the end of each experiment by their extinction following CNQX (100 μM). AMPAR responses were measured while voltage-clamping the neuron at holding potentials (3 to 5 responses/potential) between −60 and +60 mV. The rectification index (RI) was calculated as follows: $\frac{EPSC_{-60}}{-60 - E_{rev}} / \frac{EPSC_{+40}}{+40 - E_{rev}}$.

Tissue harvest and subcellular fractionation for western blot

Mice were decapitated, and the spinal cord was extruded by pressure ejection with cold saline from a 10 ml syringe with a blunt 20–22 gauge needle. The lumbar enlargement (4 mm) was first halved sagittally and then halved dorso-ventrally. The left (ipsilateral to injury) dorsal quadrant was immediately frozen with liquid nitrogen and stored at −80° C. For each sample, quadrants from 3–4 mice were pooled and homogenized in 1 ml of sucrose buffer (320 mM sucrose, 10 mM HEPES, 1 mM Na_3VO_4, 5 mM NaF, 1 mM EDTA, 1 mM EGTA, pH 7.4) using a glass-grinding vessel with rotating Teflon pestle. Each sample was processed to obtain fractions enriched for synaptic and extrasynaptic membranes (Ferrario et al., 2011; Goebel-Goody et al., 2009). This method relies on the insolubility of postsynaptic densities (PSD) and synaptic junctions in Triton X-100. The homogenate was sonicated and a 100 μl aliquot was stored at −80° C for determination of protein levels in total homogenate (TH) samples. The remainder of the homogenate was centrifuged (1,000 × g, 10 min, 4° C). The pellet (P1) was discarded and the supernatant (S1) was centrifuged (10,000 × g, 15 min, 4° C). The supernatant (S2) was discarded and the crude synaptosomal pellet (P2) was re-suspended in 0.5 ml of Triton X-100 (0.5%, v/v) detergent extraction buffer (10 mM Tris, 1 mM Na_3VO_4, 5 mM NaF, 1 mM EDTA, 1 mM EGTA, pH 7.5) using a motorized pellet-pestle mixing/grinding rod. The suspension was incubated with gentle 360° rotation (4° C, 20 min) and centrifuged (21,100 × g, 20 min, 4° C). The insoluble, synaptic fraction (PSD) was re-suspended in 75 μl of detergent extraction buffer, solubilized with 35 μl of 1% SDS. The PSD fraction was sonicated, boiled (5 min, 95° C), and stored at −80° C until protein concentration was determined.

Western Blotting

Bio-Rad DC protein assay (Hercules, CA) was used to quantify the total protein concentration of each sample. Next, equal amounts of protein (20 μg for total homogenate, 10 μg for postsynaptic density samples) were separated with SDS-polyacrylamide gel electrophoresis (Novex™ 4–12% Tris-Glycine Mini Protein Gels, Wedgewell 10-well, 1.0 mm) and transferred onto a nitrocellulose membrane. Non-specific binding was blocked using Odyssey Blocking Buffer (Licor, Lincoln, NE) for 1 h at room temperature and then

incubated overnight at 4°C with gentle rotation in primary antibody solution (Odyssey Blocking Buffer with 0.1% Tween-20) containing: anti-GluA1 (1:1000, Abcam, #ab32436), anti-GluA2 (1:1000, Millipore Sigma, #MAB397), anti-GluA4 (1:500, Millipore Sigma, #AB1508), anti-PSD95 (1:1000, Cell Signaling Technology, #2507) or anti-synaptophysin (1:2000, Abcam, #ab14692). Anti-β-actin (1:5000, Millipore Sigma, #MAB1501) was used as the loading control. After incubation, the membrane was washed with 1X TBST (3×5 min) and immersed in fluorescent secondary antibody (1:10,000 donkey anti-rabbit IgG H&L (Alexa Fluor® 680) #ab175772; 1:10,000 donkey anti-mouse IgG H&L (Alexa Fluor® 790) #ab186699), Odyssey Blocking Buffer with 0.1% Tween-20 for 1 hour. The membrane was then washed (2×5 min in 1X TBST; 2×5 min in 1X TBS) and scanned with Odyssey Imaging System V3.0 (LI-COR Biosciences, Lincoln, NE). Pixel intensity was quantified with Nikon Elements Software. Relative expression was calculated as a percentage of expression levels from uninflamed animals run on the same gel and was corrected for equal loading by dividing by β-actin intensity.

Chemicals

Fura-2 AM and Pluronic F-127 were purchased from Invitrogen (Carlsbad, CA). Glutamate was purchased from Sigma (St. Louis, MO). Naltrexone (cat #0677), naspm trihydrochloride (cat. #2766) and IEM-1460 (cat. #1636) were purchased from Tocris Bioscience (Minneapolis, MN).

Statistics

Statistical analyses for behavioral studies was performed first using a two-way ANOVA with dose and time as factors. Significant two-way ANOVA was followed by one-way ANOVA collapsed across time to area under the curve. This analysis was followed by Dunnett's multiple comparisons test (GraphPad Prism 7.03, San Diego, CA). For Ca^{2+} imaging studies, two-way ANOVA with injury as the first factor and drug as the repeated measure was used. For electrophysiology studies, groups were compared with Mann–Whitney U-test. To compare the relative abundance of protein in spinal cord samples from uninflamed compared to injured mice, one-way ANOVA followed by Dunnett's multiple comparisons test was used.

3.   Results

Spinal AMPARs retain Ca^{2+} permeability in CFA 21d mice

Incorporation of the GluA2 subunit within in the AMPAR tetramer hinders Ca^{2+} permeability and confers a linear current-voltage (I-V) relationship. By contrast, lack of the GluA2 subunit facilitates Ca^{2+} permeability and confers an inwardly-rectifying I-V relationship. To test the hypothesis that inflammation increases CP-AMPARs during CS and LCS, we performed whole-cell patch-clamp recordings in lamina II neurons obtained from CFA 3d mice (coinciding with CS) and CFA 21d mice (coinciding with LCS). We then constructed I-V curves of C-fiber stimulus-evoked, AMPAR-mediated EPSCs. Consistent with previous studies (Katano et al., 2008; Park et al., 2009; Vikman et al., 2008), CFA 3d mice exhibited a larger rectification index as compared to sham mice (RI = 1.36 ± 0.21 in sham vs. 2.12 ± 0.18 in CFA 3d mice, p = 0.041; Fig. 1A). Similarly, RI was significantly

greater in CFA 21d mice as compared to sham injured mice (RI = 1.47 ± 0.11 in sham vs 2.83 ± 0.69 in CFA 21d mice; p = 0.015, Fig. 1B).

Inflammation increases the expression of GluA1, GluA2 and GluA4 subunits in PSD

To further test the hypothesis that inflammation increases CP-AMPARs during CS and LCS, we measured the expression of AMPAR subunits in ipsilateral dorsal horn quadrants from uninflamed, CFA 2d and CFA 21d mice. In total homogenates, GluA1, GluA2 and GluA4 content was similar between uninflamed, CFA 2d, and CFA 21d mice (Fig. 2A–C, suppl Fig. 1).

PSD fractions were enriched 5.2-fold in PSD95, a specific marker of the postsynaptic density (Fig. 2D). As expected, this PSD95 fraction did not exhibit immunoreactivity to synaptophysin-I, a presynaptic marker, indicating the absence of presynaptic contaminants. Figs 2E–G illustrate that, compared to uninflamed mice, CFA increased GluA1 expression in CFA 2d mice ($F_{(2, 20)}$ = 7.80, p = 0.0031, Fig. 2E), GluA2 expression in CFA 21d mice ($F_{(2, 14)}$ = 6.56, p = 0.0098, Fig. 2F), and GluA4 expression in both CFA 2d and 21d mice ($F_{(2, 19)}$ = 6.20, p = 0.0085, Fig. 2G).

Inflammation increases sensitivity to the CP-AMPAR blocker, IEM-1460

To determine whether inflammation increases functional CP-AMPARs in CFA 21 mice we used IEM-1460, a CP-AMPAR inhibitor that works well *in vitro* (Cabanero et al., 2013). The repeatability of AMPA-evoked responses allowed for a simple within-subjects design involving two applications of AMPA (5 μM; in the presence of 10 μM cyclothiazide to prevent desensitization (Fucile et al., 2006; Kopach et al., 2013)), with 50 μM IEM-1460 included prior to and during the second application (Fig. 3). IEM-1460 did not change the peak magnitude of AMPAR-mediated Ca^{2+} transients in slices from uninflamed mice (340/380 = 0.055 ± 0.0063 for control vs. 0.048 ± 0.0047 with IEM-1460; Fig. 3). By contrast, IEM decreased peak amplitude in slices from CFA 21d mice (340/380 = 0.053 ± 0.0095 for control vs. 0.040 ± 0.0088 with IEM-1460, $F_{(1, 14)}$ = 18.18, P = 0.0008).

CP-AMPAR antagonist naspm prevents naltrexone-induced reinstatement of hyperalgesia

Inflammation induces CP-AMPAR-mediated CS and hyperalgesia within a rapid time course of hours to days (Atianjoh et al., 2010; Choi et al., 2010; Galan et al., 2004; Katano et al., 2008; Larsson and Broman, 2008; Park et al., 2009; Park et al., 2008; Vikman et al., 2008; Voitenko et al., 2004; Wigerblad et al., 2017). To test the hypothesis that CP-AMPARs maintain a longer-lasting (3 week) behavioral hypersensitivity that is masked by MOR_{CA}, we blocked MOR_{CA} with naltrexone (NTX) in the absence or presence of naspm, a CP-AMPAR inhibitor. As illustrated in Fig. 4A, mice developed mechanical hyperalgesia at 2 d post-CFA (CFA 2d) that resolved by 21 d (CFA 21d). In CFA 21d mice, but not uninflamed sham mice, NTX (1 μg, *i.t.*) reinstated mechanical hyperalgesia, consistent with our previous studies (Corder et al., 2013). Co-administration of naspm (0.01 – 10 nmol, *i.t.*) dose-dependently decreased NTX-induced mechanical hyperalgesia over the 0 – 240 min time course ($F_{(6, 47)}$ = 21.95, p < 0.0001, Dose × Time). The peak effects of naspm developed at 30–90 min after administration and then dissipated over the 240 min observation period. Further analysis of area under the curve (AUC) during the 0–240 min time interval revealed

an antihyperalgesic effect of the 1 or 10 nmol dose as compared to vehicle ($F_{(4,37)} = 6.33$, p = 0.0006, Fig. 4B).

Naltrexone increases AMPAR-mediated spinal Ca^{2+} signals in CFA 21d mice

To test the hypothesis that inflammation induces the maintenance of a long-lasting AMPAR-mediated LCS that is opposed by MOR_{CA}, we measured AMPA-evoked (5 μM, 20 s exposure) Ca^{2+} responses in lumbar slices from CFA 21d or uninflamed sham mice. As illustrated in Fig. 5A–B, NTX did not change peak AMPA-evoked Ca^{2+} transients in slices from sham mice (340/380 = 0.0413 ± 0.0037 for control vs. 0.0406 ± 0.0051 with NTX, n = 7 mice). By contrast, NTX increased transients in CFA 21 d mice (340/380 uninflamed = 0.0334 ± 0.0034 vs. NTX = 0.0402 ± 0.0038, $F_{(1,17)} = 5.44$, P = 0.032, n = 12 mice/group).

4. Discussion

Inflammation induces hyperalgesia that coincides temporally with an early increase in postsynaptic CP-AMPAR expression in the dorsal horn (Atianjoh et al., 2010; Choi et al., 2010; Galan et al., 2004; Katano et al., 2008; Larsson and Broman, 2008; Park et al., 2009; Park et al., 2008; Vikman et al., 2008; Voitenko et al., 2004; Wigerblad et al., 2017). We now show that peripheral inflammation triggers a much longer-lasting increase in the expression of synaptic CP-AMPARs, well beyond the resolution of hyperalgesia. Because CP-AMPAR antagonists reduced NTX-induced reinstatement of hyperalgesia, we conclude that this increase in CP-AMPAR accumulation persists during LCS. These pivotal findings suggest that AMPAR plasticity is maintained long-term, perhaps rendering the individual susceptible to the transition from acute to chronic pain.

Inflammation elicits an early, CP-AMPAR-mediated increase in synaptic strength

Our electrophysiological studies found that inflammation increased RI and both GluA1 and GluA4 subunits in the PSD - with no change in GluA2 subunits - at or near the peak of frank hyperalgesia. Similarly, Park and colleagues observed an increase in inwardly rectifying AMPARs and synaptic GluA1 subunit expression following CFA-induced inflammation in rat (Park et al., 2009; Park et al., 2008). We also discovered an increase in GluA4 subunits, which likely contributes to the rise in Ca^{2+} permeability and hyperalgesia. Together, these data suggest that not just the GluA1 subunit, but also the GluA4 subunit, contributes to the expression of CP-AMPARs and synaptic strength during hyperalgesia.

We report a marginal (p=0.07) increase in GluA2 subunits in the PSD fraction of CFA 2d mice. This contrasts with previous studies that reported a *decrease* in synaptic GluA2 subunits, likely associated with an increase in GluA2-lacking CP-AMPARs during inflammatory hyperalgesia (Katano et al., 2008; Park et al., 2009; Park et al., 2008). For example, Park and colleagues found that intraplantar CFA injection shifted GluA1 to, and GluA2 away from, the synaptic membrane with no change in total GluA1 or GluA2 expression (Park et al., 2009; Park et al., 2008). This disparity may be due to differences in experimental methods and reagents. First, to purify endocytosed, clathrin-coated vesicles, with subcellular fractionation methods, Park and colleagues used differential centrifugation to collect a 150 k-g spin fraction (Park et al., 2009); by contrast, we used a technique that

relies on the insolubility of PSD and synaptic junctions in Triton X-100, a method that enriches the PSD fraction with PSD-95 and without contamination of the presynaptic protein synaptophysin. Second, we performed our studies in mouse, while Park et al. used rat, raising the possibility of a species difference in AMPAR regulation.

Does Inflammation elicit a long-lasting, CP-AMPAR-mediated increase in synaptic strength?

We provide for the first time several lines of evidence that suggest that inflammation CP-AMPAR-mediated increases in synaptic strength in lamina II neurons of the spinal cord, well after the resolution of hyperalgesia. First, our electrophysiology studies revealed that inflammation increased inward rectification of AMPAR-mediated EPSCs, a shift that persisted to 21 d after injury. Second, our slice Ca^{2+} imaging studies found that the CP-AMPAR antagonist, IEM-1460, produced greater inhibition of AMPA-mediated Ca^{2+} signaling in lamina II neurons in CFA 21d mice as compared to uninflamed mice. Future studies are needed to determine whether this increased sensitivity is due to an increase in CP-AMPAR insertion, or to ion channel characteristics (e.g. open probability or open time) as previously suggested (Banke et al., 2000; Derkach et al., 1999).

Our biochemical data indicated an increase in both GluA2 and GluA4 AMPAR subunits at the dorsal horn PSD during the 21 d timepoint that is reflective of LCS. Since there were no changes in total GluA2 expression at any timepoint, we conclude that subunit trafficking, rather than protein synthesis, underlies the observed increase in postsynaptic AMPAR subunits.

Our data reveal that inflammation induced a long-lasting increase in the PSD of CFA 21d mice not only in GluA4 expression, but also in GluA2 expression. We propose two explanations for our finding that inflammation increases AMPAR Ca^{2+} permeability despite increases in GluA2. First, inflammation might increase CP-AMPARs and CI-AMPARs in the same cell, with the net result of increased calcium permeability. In this scenario, the CP-AMPARs would be comprised of homomeric GluA4, as observed following morphine treatment in a model of opioid-induced hyperalgesia (Cabanero et al., 2013). These CP-AMPARs should contribute to synaptic transmission unhindered by CI-AMPARs comprised of GluA2/GluA1 dimers or GluA2/GluA4 dimers.

As a second explanation for our findings that inflammation increases AMPAR Ca^{2+} permeability despite increases in GluA2, we speculate that inflammation increases GluA4-containing CP-AMPARs in pain excitatory neurons and increases GluA2-containing CI-AMPARs in pain inhibitory neurons; both of which increase nociceptive transmission. Previous studies suggest that painful injury can regulate AMPAR function and subunit expression in specific DH neuron populations. For example, in the CCI model of neuropathic pain, Chen and colleagues demonstrated that injury selectively decreased both single channel conductance and decreased sensitivity to inhibition of synaptic AMPAR currents by IEM-1460 in inhibitory (tonic firing), but not in excitatory (delayed firing) rat lamina II neurons (Chen et al., 2016a). Although we suggest an increase in CI-AMPARs in pain inhibitory neurons during LCS (while CCI produced a decrease in CP-AMPARs),

specific AMPAR regulatory mechanisms may depend on factors including injury model and/or time point.

Perhaps more important than the excitatory or inhibitory nature of the cell is the circuit that injury activates. For example, somatostatin (SOM)-expressing neurons in the DH are pronociceptive; their activation is required for the sensation of mechanical pain (Duan et al., 2014) while parvalbumin (PV)-expressing neurons contribute to antinociceptive neurotransmission (Boyle et al., 2017; Petitjean et al., 2015). We speculate a scenario where inflammation increases CP-AMPARs (i.e. GluA4 subunit expression) specifically in pronociceptive SOM neurons but not in PV neurons during LCS. Likewise, we would predict a gain of GluA2 subunits and therefore CI-AMPARs in anti-nociceptive PV but not SOM neurons. Current understanding of the neuronal circuitry in the DH is limited. However, the recent development of molecular genetic techniques for altering neuronal function *in vivo* is resulting in a dramatic improvement in our understanding not only of the neuronal properties, but to the contribution to nociceptive processing at the spinal level. These ideas cannot be resolved with western blot studies. Instead, further studies are needed to determine AMPAR subunit composition in dorsal horn neuronal populations and thus resolve the exact role of specific GluA subunits during LCS.

Spinal CP-AMPARs expressed during LCS are masked by MOR$_{CA}$

We previously demonstrated that inflammatory pain is associated with the establishment of a compensatory endogenous analgesia due to MOR constitutive activity (MOR$_{CA}$) in the dorsal horn (Corder et al., 2013). For example, disruption of MOR$_{CA}$ with an inverse agonist increased glutamate-evoked spinal Ca^{2+} signaling *ex vivo* in spinal cord slices when tested 21 d after CFA. We have previously established that AMPARs mediate the majority of Ca^{2+} response to glutamate (Doolen et al., 2012). Here, we show that AMPAR-mediated Ca^{2+} signaling increased in the presence of NTX at 21 d post-injury, confirming an AMPAR contribution to LCS. Naspm dose-dependently reversed NTX-induced reinstatement of mechanical hyperalgesia. This effect is not likely due to side effects and/or sedation, as naspm had no effect on mechanical thresholds in sham-injured mice, and previous studies indicate a lack of effect on motor function after i.t. naspm administration (Cabanero et al., 2013).

Inflammation increases synaptic strength in postsynaptic dorsal horn neurons

Our electrophysiological studies revealed an increase in RI in recordings from postsynaptic lamina II cells, indicating an increase in postsynaptic CP-AMPARs. In support of AMPAR-mediated synaptic strengthening at postsynaptic sites, our biochemical data demonstrated that inflammation increased GluA4 subunit expression in fractions enriched in postsynaptic density. Thus, we argue that inflammation increases Ca^{2+} signaling by driving plasticity at postsynaptic lamina II neurons, either by increasing the activity of pronociceptive pathways, decreasing the activity of antinociceptive pathways, or both. However, our studies do not rule out a contribution of either presynaptic or extrasynapatic AMPARs. Indeed, peripheral presynaptic CP-AMPARs can contribute to inflammatory pain (Gangadharan et al., 2011). Our studies were not designed to isolate this mechanism, as bath application of AMPA likely overrode plasticity at presynaptic glutamatergic terminals. Furthermore, numerous *in vitro*

and *in vivo* studies demonstrate that extrasynaptic AMPARs are highly mobile at the plasma membrane and rapidly and continuously move between the membrane surface and intracellular compartments by exocytosis and endocytosis (Bredt and Nicoll, 2003; Malinow and Malenka, 2002) as well as laterally diffusing to and from synaptic sites (Bats et al., 2007; Borgdorff and Choquet, 2002; Choquet and Triller, 2003; Cognet et al., 2006). While the contribution of extrasynaptic AMPARs to synaptic transmission is not fully understood, extrasynaptic AMPAR trafficking participates in the maintenance of persistent inflammatory pain (Kopach et al., 2011; Kopach and Voitenko, 2013), and so may also operate in the setting of LCS.

Inflammation increases postsynaptic GluA1 during early hyperalgesia but not during LCS.

Tissue injury changes the equilibrium of synaptic and extrasynaptic AMPAR subunits in dorsal horn neurons. For example, intraplantar CFA increased postsynaptic GluA1 AMPAR subunits in the superficial dorsal horn 24 h after injection (Katano et al., 2008; Park et al., 2008). Likewise, intraplantar injection of inflammogens including capsaicin (Larsson and Broman, 2008), formalin (Pezet et al., 2008) carrageenan (Choi et al., 2010; Wigerblad et al., 2017) and intracolonic capsaicin (Galan et al., 2004) produced immediate increases in membrane GluA1 AMPAR subunits in the superficial dorsal horn at 10–180 min after injection. Our results are consistent with these findings: CFA increased postsynaptic GluA1 at 2 days post-injection. And for the first time, our studies extend this analysis to much later timepoints: by 21 d post-injury, PSD GluA1 expression returned to baseline levels as measured in uninflamed mice. We suggest that CFA increases postsynaptic GluA1 expression in a temporal manner that correlates with hyperalgesia. Specifically, we argue that inflammation increases GluA1-mediated synaptic strengthening during the early hyperalgesia phase, but not during the remission phase of LCS.

Inflammation increases postsynaptic GluA4

Only a few studies describe the contribution of the GluA4 subunit to CNS function. One study suggested that PKA-driven synaptic insertion of GluA4 AMPA receptors is the predominant mechanism for synaptic strengthening in hippocampus (Kessels and Malinow, 2009; Zhu et al., 2000). GluA4 subunits are also essential for auditory processing (Rubio et al., 2017) and contribute to memory consolidation (Ganea et al., 2015). Here, we found that CFA-induced inflammation increased synaptic GluA4 subunit expression near the peak of hyperalgesia. This is consistent with an emerging relationship between membrane GluA4 spinal sensitization and nociception during hyperalgesic states. For example, Svensson, Sorkin and colleagues reported that carrageenan-induced inflammation increased GluA4 subunit expression in the plasma membrane, and also increased synaptic GluA1 (Wigerblad et al., 2017). Also, nociceptive neurons that develop CP-AMPA receptors as GluA4 homomers were identified in laminae III-IV during opioid-induced hyperalgesia (12 hours after discontinuing morphine) (Cabanero et al., 2013). Interestingly, we found that CFA-induced inflammation increased synaptic GluA4 at both 2 and 21 d after injury. This suggests that GluA4 subunits may contribute to central sensitization during early hyperalgesia as well as during LCS.

Spinal AMPAR plasticity, LCS, and MOR$_{CA}$: Molecular mechanisms

Our behavioral and Ca^{2+} imaging data using NTX model of LCS demonstrate a long-lasting increase in CP-AMPARs that lasts well after inflammatory pain. Although the molecular mechanisms that drive this long-lasting AMPAR plasticity during LCS are unknown, several lines of evidence suggest MOR$_{CA}$ inhibits nociceptive AMPAR signaling by post-transcriptional mechanisms. First, MOR inverse agonists elicited reinstatement of LCS (behavioral and Ca^{2+} signaling) within 15 minutes of administration. Second, our western blot data indicated that the CP-AMPAR machinery is expressed during LCS; inflammation increased postsynaptic GluA4 subunits in CFA 21d mice. Third, inflammation increased sensitivity to IEM-1460 in CFA 21d mice. We suggest that inflammation leads to long-lasting changes in pro-nociceptive AMPAR function that is opposed by anti-nociceptive MOR$_{CA}$.

Previous studies suggest that inhibition of NMDA, AC1, PKA, PKC and PI3 kinase activation prevents hyperalgesia and CP-AMPAR signaling in the presence of inflammatory injury (Liu et al., 2015; Lu et al., 2003; Park et al., 2009; Wigerblad et al., 2017). Although we have established that MOR$_{CA}$ disruption reinstates an NMDA-AC1-PKA signaling pathway during LCS (Corder et al., 2013), future studies are necessary to determine whether one or more of these molecules drive AMPAR plasticity during LCS.

What drives the long-lasting injury-induced increase in GluA2 and GluA4 subunit expression? We believe that an important clue comes from a model of incubated drug craving. For example, Wolf and colleagues recently reported that NMDARs contribute to long-term AMPAR plasticity in the nucleus accumbens. An initial increase in GluN2B-containing receptors during the first week of withdrawal occurs followed 1–2 weeks later by the appearance of NMDARs that contain the GluN3 subunit along with GluN2B; and these steps were necessary for accumulation of CP-AMPARs and drug seeking (Dong et al., 2017). Based on the idea that incubated craving and LCS share features of long-lasting AMPAR plasticity, we suggest additional studies to determine the potential contribution of NMDA subunit dysregulation to AMPAR plasticity in LCS.

In addition to MOR$_{CA}$, other receptors such as alpha-2 adrenergic and neuropeptide Y (NPY) Y1 receptor (Y1R) mask inflammation- or nerve injury-induced LCS (De Felice et al., 2011; Solway et al., 2011; Walwyn et al., 2016). For example, studies from our laboratory used conditional knockdown of NPY and NPY Y1R and Y2R antagonists to demonstrate tonic inhibition of chronic pain by NPY (Solway et al., 2011). As NPY suppresses epileptiform discharges via an increase in synaptic GluA2 subunit expression in rat hippocampal neurons (Bu et al., 2017), future studies are warranted to determine whether Y1R analgesic systems tonically suppress CP-AMPAR function during LCS.

Clinical/translational relevance

We reported that naloxone reinstated pain hypersensitivity when given weeks after a mild thermal injury in 4 out of 12 subjects, suggesting that MOR$_{CA}$ masks LCS in humans (Pereira et al., 2015; Springborg et al., 2016). If larger studies confirm this finding, then it is plausible that CP-AMPAR activity predisposes patients to the transition from acute to

chronic pain. Although broad-spectrum, competitive AMPAR antagonists reduced muscle tone and caused sedation (Hao and Xu, 1996), broad-spectrum, noncompetitive, AMPAR antagonists are FDA approved for the treatment of epilepsy (Faulkner and Burke, 2013) and are being investigated for other CNS conditions (Keppel Hesselink, 2017). Together with the recent finding that CP-AMPAR inhibitors such as IEM-1460 alleviated the early phase of inflammatory hyperalgesia in rodents (Kopach et al., 2016), our results promote the selective targeting of CP-AMPARs as a new pharmacotherapy for chronic inflammatory pain states.

Supplementary Material

Refer to Web version on PubMed Central for supplementary material.

Acknowledgements

Abbreviations

AC1	Adenylyl cyclase I
AMPA	α-amino-3-hydroy-5-methyl-4-isoxazolepropionic acid
AMPAR	AMPA receptor
CFA	complete Freund's adjuvant
CFA 21 d	mice tested 21 d after injection of CFA
CP-AMPAR	Ca^{2+}-permeable AMPAR
CI-AMPAR	Ca^{2+}-impermeable AMPAR
CS	central sensitization
DH	dorsal horn
EPSC	excitatory post-synaptic current
LCS	latent central sensitization
MOR$_{CA}$	mu opioid receptor constitutive activity
NMDA	N-methyl-D-aspartic acid
NTX	naltrexone
PKA	protein kinase A
PKC	protein kinase C
PI3	phosphatidylinositol 3
PSD	postsynaptic density

| **ROIs** | Regions of interest |
| **TH** | total homogenate |

References

Atianjoh FE, Yaster M, Zhao X, Takamiya K, Xia J, Gauda EB, Huganir RL, Tao YX, 2010 Spinal cord protein interacting with C kinase 1 is required for the maintenance of complete Freund's adjuvant-induced inflammatory pain but not for incision-induced post-operative pain. Pain 151, 226–234. [PubMed: 20696523]

Banke TG, Bowie D, Lee H, Huganir RL, Schousboe A, Traynelis SF, 2000 Control of GluR1 AMPA receptor function by cAMP-dependent protein kinase. J Neurosci 20, 89–102. [PubMed: 10627585]

Bats C, Groc L, Choquet D, 2007 The interaction between Stargazin and PSD-95 regulates AMPA receptor surface trafficking. Neuron 53, 719–734. [PubMed: 17329211]

Borgdorff AJ, Choquet D, 2002 Regulation of AMPA receptor lateral movements. Nature 417, 649–653. [PubMed: 12050666]

Boyle KA, Gutierrez-Mecinas M, Polgar E, Mooney N, O'Connor E, Furuta T, Watanabe M, Todd AJ, 2017 A quantitative study of neurochemically defined populations of inhibitory interneurons in the superficial dorsal horn of the mouse spinal cord. Neuroscience 363, 120–133. [PubMed: 28860091]

Bredt DS, Nicoll RA, 2003 AMPA receptor trafficking at excitatory synapses. Neuron 40, 361–379. [PubMed: 14556714]

Bu W, Zhao WQ, Li WL, Dong CZ, Zhang Z, Li QJ, 2017 Neuropeptide Y suppresses epileptiform discharges by regulating AMPA receptor GluR2 subunit in rat hippocampal neurons. Mol Med Rep 16, 387–395. [PubMed: 28498410]

Burnashev N, Monyer H, Seeburg PH, Sakmann B, 1992 Divalent ion permeability of AMPA receptor channels is dominated by the edited form of a single subunit. Neuron 8, 189–198. [PubMed: 1370372]

Cabanero D, Baker A, Zhou S, Hargett GL, Irie T, Xia Y, Beaudry H, Gendron L, Melyan Z, Carlton SM, Moron JA, 2013 Pain after discontinuation of morphine treatment is associated with synaptic increase of GluA4-containing AMPAR in the dorsal horn of the spinal cord. Neuropsychopharmacology 38, 1472–1484. [PubMed: 23403695]

Campillo A, Cabanero D, Romero A, Garcia-Nogales P, Puig MM, 2011 Delayed postoperative latent pain sensitization revealed by the systemic administration of opioid antagonists in mice. Eur J Pharmacol 657, 89–96. [PubMed: 21300053]

Chaplan SR, Bach FW, Pogrel JW, Chung JM, Yaksh TL, 1994 Quantitative assessment of tactile allodynia in the rat paw. J Neurosci Methods 53, 55–63. [PubMed: 7990513]

Chen SR, Zhou HY, Byun HS, Pan HL, 2013 Nerve injury increases GluA2-lacking AMPA receptor prevalence in spinal cords: functional significance and signaling mechanisms. J Pharmacol Exp Ther 347, 765–772. [PubMed: 24030012]

Chen Y, Derkach VA, Smith PA, 2016a Corrigendum to "Loss of Ca2+-permeable AMPA receptors in synapses of tonic firing substantia gelatinosa neurons in the chronic constriction injury model of neuropathic pain" [Experimental Neurology 279 (2016) 168–177]. Exp Neurol 286, 150. [PubMed: 27574732]

Chen Y, Derkach VA, Smith PA, 2016b Loss of Ca(2+)-permeable AMPA receptors in synapses of tonic firing substantia gelatinosa neurons in the chronic constriction injury model of neuropathic pain. Exp Neurol 279, 168–177. [PubMed: 26948545]

Choi JI, Svensson CI, Koehrn FJ, Bhuskute A, Sorkin LS, 2010 Peripheral inflammation induces tumor necrosis factor dependent AMPA receptor trafficking and Akt phosphorylation in spinal cord in addition to pain behavior. Pain 149, 243–253. [PubMed: 20202754]

Choquet D, Triller A, 2003 The role of receptor diffusion in the organization of the postsynaptic membrane. Nat Rev Neurosci 4, 251–265. [PubMed: 12671642]

Cognet L, Groc L, Lounis B, Choquet D, 2006. Multiple routes for glutamate receptor trafficking: surface diffusion and membrane traffic cooperate to bring receptors to synapses. Sci STKE 2006, pe13. [PubMed: 16552090]

Corder G, Doolen S, Donahue RR, Winter MK, Jutras BL, He Y, Hu X, Wieskopf JS, Mogil JS, Storm DR, Wang ZJ, McCarson KE, Taylor BK, 2013 Constitutive mu-opioid receptor activity leads to long-term endogenous analgesia and dependence. Science 341, 1394–1399. [PubMed: 24052307]

De Felice M, Sanoja R, Wang R, Vera-Portocarrero L, Oyarzo J, King T, Ossipov MH, Vanderah TW, Lai J, Dussor GO, Fields HL, Price TJ, Porreca F, 2011 Engagement of descending inhibition from the rostral ventromedial medulla protects against chronic neuropathic pain. Pain 152, 2701–2709. [PubMed: 21745713]

Derkach V, Barria A, Soderling TR, 1999 Ca2+/calmodulin-kinase II enhances channel conductance of alpha-amino-3-hydroxy-5-methyl-4-isoxazolepropionate type glutamate receptors. Proc Natl Acad Sci U S A 96, 3269–3274. [PubMed: 10077673]

Dong Y, Taylor JR, Wolf ME, Shaham Y, 2017 Circuit and Synaptic Plasticity Mechanisms of Drug Relapse. J Neurosci 37, 10867–10876. [PubMed: 29118216]

Doolen S, Blake CB, Smith BN, Taylor BK, 2012 Peripheral nerve injury increases glutamate-evoked calcium mobilization in adult spinal cord neurons. Mol Pain 8, 56. [PubMed: 22839304]

Duan B, Cheng L, Bourane S, Britz O, Padilla C, Garcia-Campmany L, Krashes M, Knowlton W, Velasquez T, Ren X, Ross S, Lowell BB, Wang Y, Goulding M, Ma Q, 2014 Identification of spinal circuits transmitting and gating mechanical pain. Cell 159, 1417–1432. [PubMed: 25467445]

Fairbanks CA, 2003 Spinal delivery of analgesics in experimental models of pain and analgesia. Adv Drug Deliv Rev 55, 1007–1041. [PubMed: 12935942]

Faulkner MA, Burke RA, 2013 Safety profile of two novel antiepileptic agents approved for the treatment of refractory partial seizures: ezogabine (retigabine) and perampanel. Expert Opin Drug Saf.

Ferrario CR, Loweth JA, Milovanovic M, Wang X, Wolf ME, 2011 Distribution of AMPA receptor subunits and TARPs in synaptic and extrasynaptic membranes of the adult rat nucleus accumbens. Neurosci Lett 490, 180–184. [PubMed: 21182898]

Fucile S, Miledi R, Eusebi F, 2006 Effects of cyclothiazide on GluR1/AMPA receptors. Proc Natl Acad Sci U S A 103, 2943–2947. [PubMed: 16473938]

Galan A, Laird JM, Cervero F, 2004 In vivo recruitment by painful stimuli of AMPA receptor subunits to the plasma membrane of spinal cord neurons. Pain 112, 315–323. [PubMed: 15561387]

Ganea DA, Dines M, Basu S, Lamprecht R, 2015 The Membrane Proximal Region of AMPA Receptors in Lateral Amygdala is Essential for Fear Memory Formation. Neuropsychopharmacology 40, 2727–2735. [PubMed: 25915472]

Gangadharan V, Wang R, Ulzhofer B, Luo C, Bardoni R, Bali KK, Agarwal N, Tegeder I, Hildebrandt U, Nagy GG, Todd AJ, Ghirri A, Haussler A, Sprengel R, Seeburg PH, MacDermott AB, Lewin GR, Kuner R, 2011 Peripheral calcium-permeable AMPA receptors regulate chronic inflammatory pain in mice. J Clin Invest 121, 1608–1623. [PubMed: 21383497]

Goebel-Goody SM, Davies KD, Alvestad Linger RM, Freund RK, Browning MD, 2009 Phospho-regulation of synaptic and extrasynaptic N-methyl-d-aspartate receptors in adult hippocampal slices. Neuroscience 158, 1446–1459. [PubMed: 19041929]

Hao JX, Xu XJ, 1996 Treatment of a chronic allodynia-like response in spinally injured rats: effects of systemically administered excitatory amino acid receptor antagonists. Pain 66, 279–285. [PubMed: 8880851]

Hollmann M, Hartley M, Heinemann S, 1991 Ca2+ permeability of KA-AMPA--gated glutamate receptor channels depends on subunit composition. Science 252, 851–853. [PubMed: 1709304]

Katano T, Furue H, Okuda-Ashitaka E, Tagaya M, Watanabe M, Yoshimura M, Ito S, 2008 N-ethylmaleimide-sensitive fusion protein (NSF) is involved in central sensitization in the spinal cord through GluR2 subunit composition switch after inflammation. Eur J Neurosci 27, 3161–3170. [PubMed: 18598260]

Keinanen K, Wisden W, Sommer B, Werner P, Herb A, Verdoorn TA, Sakmann B, Seeburg PH, 1990 A family of AMPA-selective glutamate receptors. Science 249, 556–560. [PubMed: 2166337]

Keppel Hesselink JM, 2017 NS1209/SPD 502, A Novel Selective AMPA Antagonist for Stroke, Neuropathic Pain or Epilepsy? Drug Development Lessons Learned. Drug Dev Res 78, 75–80. [PubMed: 28195646]

Kessels HW, Malinow R, 2009 Synaptic AMPA receptor plasticity and behavior. Neuron 61, 340–350. [PubMed: 19217372]

Kopach O, Kao SC, Petralia RS, Belan P, Tao YX, Voitenko N, 2011 Inflammation alters trafficking of extrasynaptic AMPA receptors in tonically firing lamina II neurons of the rat spinal dorsal horn. Pain 152, 912–923. [PubMed: 21282008]

Kopach O, Krotov V, Belan P, Voitenko N, 2015 Inflammatory-induced changes in synaptic drive and postsynaptic AMPARs in lamina II dorsal horn neurons are cell-type specific. Pain 156, 428–438. [PubMed: 25599231]

Kopach O, Krotov V, Goncharenko J, Voitenko N, 2016 Inhibition of Spinal Ca(2+)-Permeable AMPA Receptors with Dicationic Compounds Alleviates Persistent Inflammatory Pain without Adverse Effects. Front Cell Neurosci 10, 50. [PubMed: 26973464]

Kopach O, Viatchenko-Karpinski V, Atianjoh FE, Belan P, Tao YX, Voitenko N, 2013 PKCalpha is required for inflammation-induced trafficking of extrasynaptic AMPA receptors in tonically firing lamina II dorsal horn neurons during the maintenance of persistent inflammatory pain. J Pain 14, 182–192. [PubMed: 23374940]

Kopach O, Voitenko N, 2013 Extrasynaptic AMPA receptors in the dorsal horn: evidence and functional significance. Brain Res Bull 93, 47–56. [PubMed: 23194665]

Larsson M, Broman J, 2008 Translocation of GluR1-containing AMPA receptors to a spinal nociceptive synapse during acute noxious stimulation. J Neurosci 28, 7084–7090. [PubMed: 18614677]

Liu SB, Zhang MM, Cheng LF, Shi J, Lu JS, Zhuo M, 2015 Long-term upregulation of cortical glutamatergic AMPA receptors in a mouse model of chronic visceral pain. Mol Brain 8, 76. [PubMed: 26585043]

Lu HC, She WC, Plas DT, Neumann PE, Janz R, Crair MC, 2003 Adenylyl cyclase I regulates AMPA receptor trafficking during mouse cortical 'barrel' map development. Nat Neurosci 6, 939–947. [PubMed: 12897788]

Luo C, Seeburg PH, Sprengel R, Kuner R, 2008 Activity-dependent potentiation of calcium signals in spinal sensory networks in inflammatory pain states. Pain 140, 358–367. [PubMed: 18926636]

Malinow R, Malenka RC, 2002 AMPA receptor trafficking and synaptic plasticity. Annu Rev Neurosci 25, 103–126. [PubMed: 12052905]

Nakatsuka T, Ataka T, Kumamoto E, Tamaki T, Yoshimura M, 2000 Alteration in synaptic inputs through C-afferent fibers to substantia gelatinosa neurons of the rat spinal dorsal horn during postnatal development. Neuroscience 99, 549–556. [PubMed: 11029546]

Park JS, Voitenko N, Petralia RS, Guan X, Xu JT, Steinberg JP, Takamiya K, Sotnik A, Kopach O, Huganir RL, Tao YX, 2009 Persistent inflammation induces GluR2 internalization via NMDA receptor-triggered PKC activation in dorsal horn neurons. J Neurosci 29, 3206–3219. [PubMed: 19279258]

Park JS, Yaster M, Guan X, Xu JT, Shih MH, Guan Y, Raja SN, Tao YX, 2008 Role of spinal cord alpha-amino-3-hydroxy-5-methyl-4-isoxazolepropionic acid receptors in complete Freund's adjuvant-induced inflammatory pain. Mol Pain 4, 67. [PubMed: 19116032]

Pereira MP, Donahue RR, Dahl JB, Werner M, Taylor BK, Werner MU, 2015 Endogenous Opioid-Masked Latent Pain Sensitization: Studies from Mouse to Human. PloS one 10, e0134441. [PubMed: 26305798]

Petitjean H, Pawlowski SA, Fraine SL, Sharif B, Hamad D, Fatima T, Berg J, Brown CM, Jan LY, Ribeiro-da-Silva A, Braz JM, Basbaum AI, Sharif-Naeini R, 2015 Dorsal Horn Parvalbumin Neurons Are Gate-Keepers of Touch-Evoked Pain after Nerve Injury. Cell Rep 13, 1246–1257. [PubMed: 26527000]

Pezet S, Marchand F, D'Mello R, Grist J, Clark AK, Malcangio M, Dickenson AH, Williams RJ, McMahon SB, 2008 Phosphatidylinositol 3-kinase is a key mediator of central sensitization in painful inflammatory conditions. J Neurosci 28, 4261–4270. [PubMed: 18417706]

Rubio ME, Matsui K, Fukazawa Y, Kamasawa N, Harada H, Itakura M, Molnar E, Abe M, Sakimura K, Shigemoto R, 2017 The number and distribution of AMPA receptor channels containing fast kinetic GluA3 and GluA4 subunits at auditory nerve synapses depend on the target cells. Brain Struct Funct 222, 3375–3393. [PubMed: 28397107]

Solway B, Bose SC, Corder G, Donahue RR, Taylor BK, 2011 Tonic inhibition of chronic pain by neuropeptide Y. Proc Natl Acad Sci U S A 108, 7224–7229. [PubMed: 21482764]

Springborg AD, Jensen EK, Taylor BK, Werner MU, 2016 Effects of target-controlled infusion of high-dose naloxone on pain and hyperalgesia in a human thermal injury model: a study protocol: A randomized, double-blind, placebo-controlled, crossover trial with an enriched design. Medicine (Baltimore) 95, e5336. [PubMed: 27861362]

Taylor BK, Corder G, 2014 Endogenous analgesia, dependence, and latent pain sensitization. Current topics in behavioral neurosciences 20, 283–325. [PubMed: 25227929]

Torsney C, MacDermott AB, 2006 Disinhibition opens the gate to pathological pain signaling in superficial neurokinin 1 receptor-expressing neurons in rat spinal cord. J Neurosci 26, 1833–1843. [PubMed: 16467532]

Vikman KS, Rycroft BK, Christie MJ, 2008 Switch to Ca2+-permeable AMPA and reduced NR2B NMDA receptor-mediated neurotransmission at dorsal horn nociceptive synapses during inflammatory pain in the rat. J Physiol 586, 515–527. [PubMed: 18033811]

Voitenko N, Gerber G, Youn D, Randic M, 2004 Peripheral inflamation-induced increase of AMPA-mediated currents and Ca2+ transients in the presence of cyclothiazide in the rat substantia gelatinosa neurons. Cell Calcium 35, 461–469. [PubMed: 15003855]

Walwyn WM, Chen W, Kim H, Minasyan A, Ennes HS, McRoberts JA, Marvizon JC, 2016 Sustained Suppression of Hyperalgesia during Latent Sensitization by mu-, delta-, and kappa-opioid receptors and alpha2A Adrenergic Receptors: Role of Constitutive Activity. J Neurosci 36, 204–221. [PubMed: 26740662]

Wigerblad G, Huie JR, Yin HZ, Leinders M, Pritchard RA, Koehrn FJ, Xiao WH, Bennett GJ, Huganir RL, Ferguson AR, Weiss JH, Svensson CI, Sorkin LS, 2017 Inflammation-induced GluA1 trafficking and membrane insertion of Ca2+ permeable AMPA receptors in dorsal horn neurons is dependent on spinal tumor necrosis factor, PI3 kinase and protein kinase A. Exp Neurol 293, 144–158. [PubMed: 28412220]

Zhu JJ, Esteban JA, Hayashi Y, Malinow R, 2000 Postnatal synaptic potentiation: delivery of GluR4-containing AMPA receptors by spontaneous activity. Nat Neurosci 3, 1098–1106. [PubMed: 11036266]
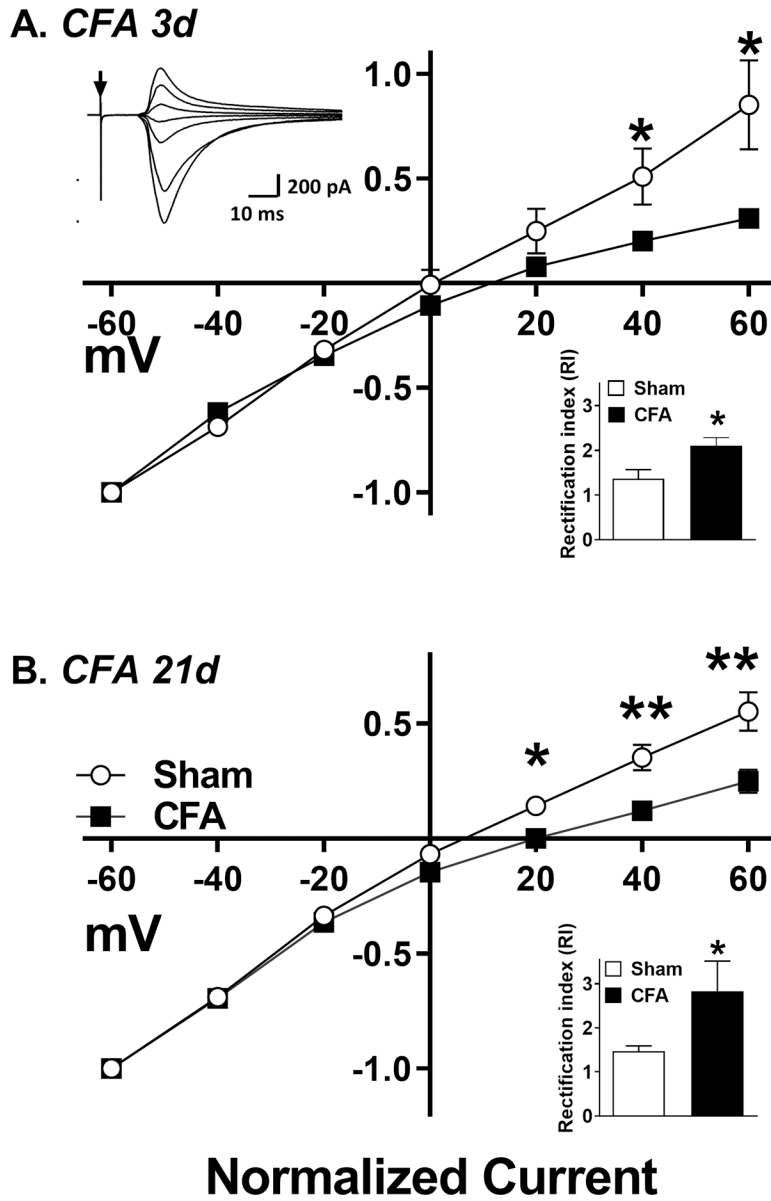
Figure 1. AMPA receptors retain Ca^{2+} permeability in CFA 21d mice.
EPSCs were recorded at different membrane potentials from −60 mV to +60 mV in 20 mV steps. The *I-V* curves represent the C-fiber mediated, evoked peak EPSCs measured at (A) 3 d and (B) 21 d after CFA injury. Inset, top-left; example plot of AMPAR mediated EPSCs at various membrane potentials. Arrow marks time of DRS. Inset, bottom-right; RI for saline vs. CFA treated animals calculated as described in methods. Data represent mean ± SEM. N = 5–6 mice/group. *p<0.05, **p<0.01 vs sham group.
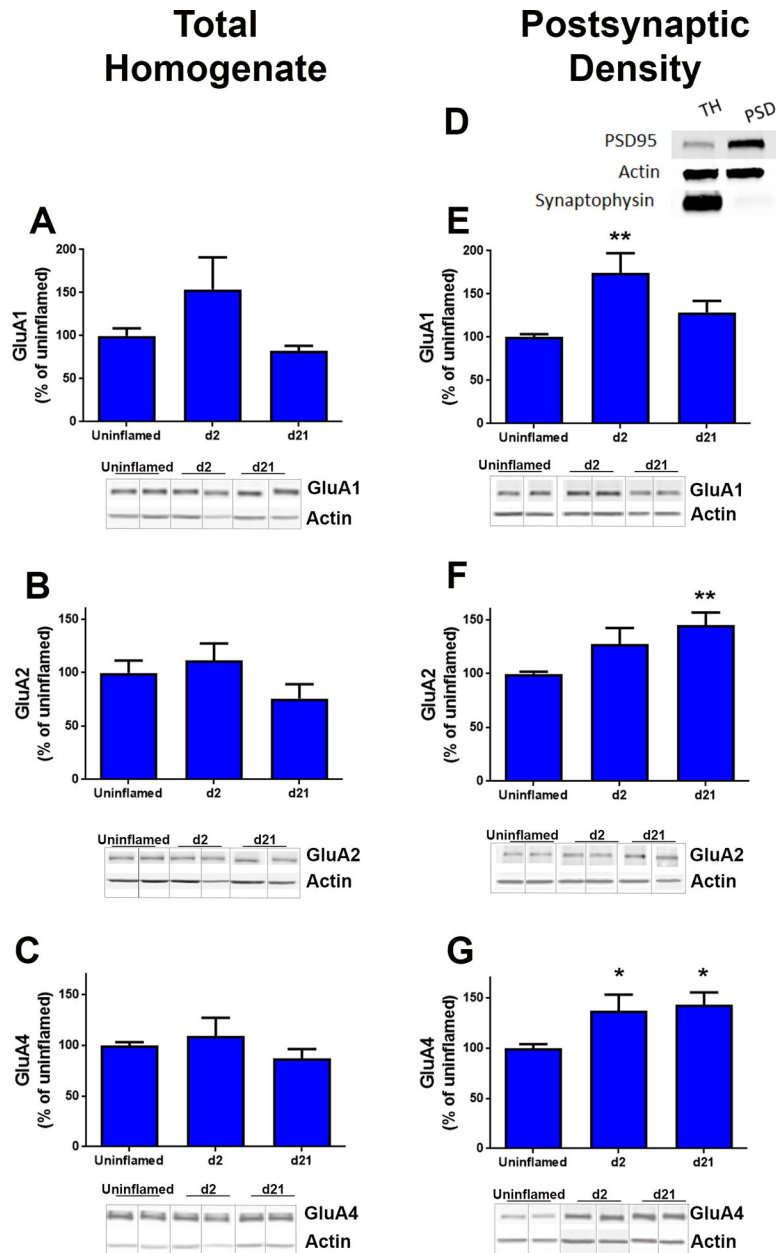
Figure 2. Inflammation increases the expression of GluA1, GluA2 and GluA4 subunits in PSD. Western blots were performed using the following primary antibodies; (A, E) anti-GluA1, (B, F) anti-GluA2, and (C, G) anti-GluA4. Representative blots are shown below each graph. D. Subcellular fractionation: A representative western blot shows enrichment of PSD-95 (postsynaptic marker) and the absence of synaptophysin-I (presynaptic marker) in postsynaptic density fractions from dorsal horns. Densitometry was performed to quantify pixel density in each western as a measure of subunit expression at d0, d2 and d21 post-CFA injection. Quantification was performed relative to β-actin levels. Ipsilateral dorsal horns from lumbar L3/L4 spinal cords of four mice were pooled to obtain each individual sample. * p<0.05 n= 4–7 samples per time point. All blots and data analyses are available in Supplemental Figure 1.

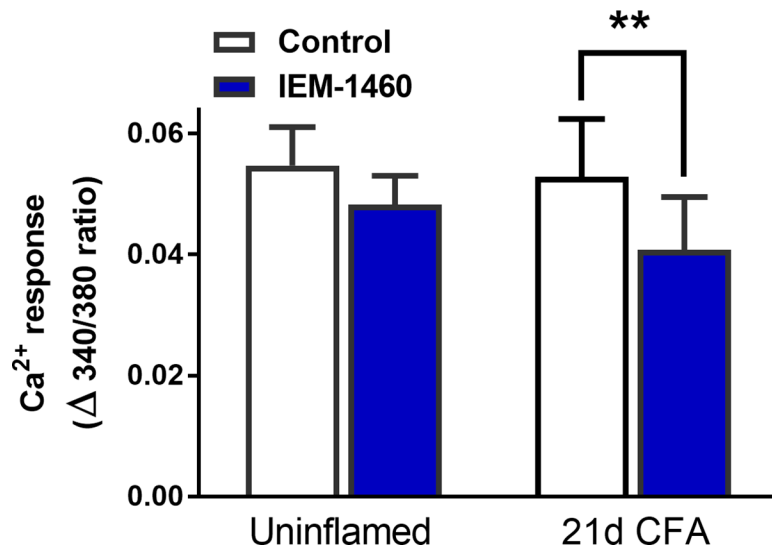**Figure 3. Inflammatory injury increases sensitivity to the Ca^{2+} permeable-AMPAR blocker, IEM-1460.**

IEM-1460 (50 μM, 10 min exposure) decreased AMPA-evoked $[Ca^{2+}]_i$ in dorsal horn of CFA 21d but not uninflamed mice. **p<0.01 vs control Ca^{2+} response to AMPA (Dunnett's post-hoc test following 2-way ANOVA with repeated measures). Data represent mean ± SEM, N = 8 mice/group.
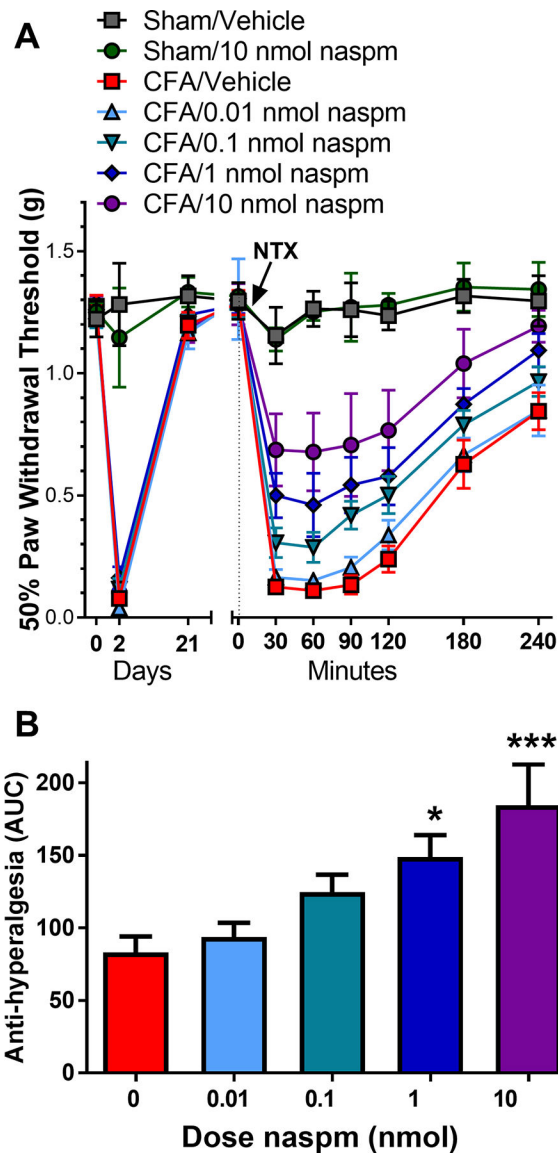
Figure 4. CP-AMPAR antagonist naspm prevents naltrexone-induced reinstatement of hyperalgesia.

A. Mice that received hindpaw CFA (5 μl, intraplantar) developed a mechanical hyperalgesia at 2 d that resolved within 21 d. NTX (1 μg, *i.t.*) reinstated hyperalgesia when administered 21 d after intraplantar injection of CFA but not saline (sham). Co-administration of naspm (0–1 nmol, *i.t.*) dose-dependently reduced NTX-mediated reinstatement of hyperalgesia. B. Effect of naspm was calculated as area under the curve (area under data points from 30–240 min; AUC). Data represent mean ± SEM. N = 6–9 mice/group. *p<0.05, ***p<0.001 vs vehicle/CFA group (0 nmol naspm; depicted in red).
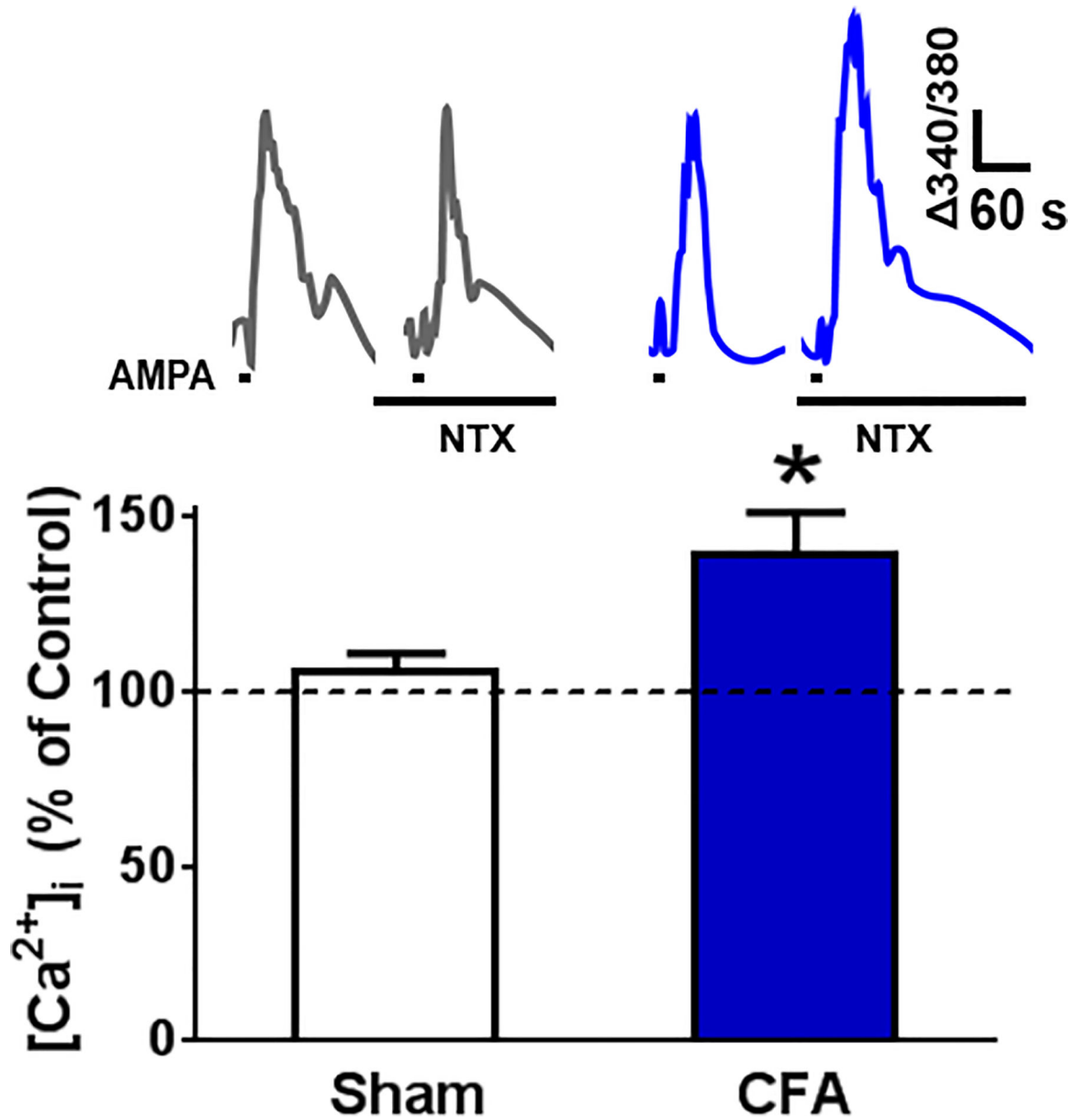
Figure 5. Naltrexone increases AMPAR-mediated spinal Ca^{2+} signals in CFA 21d mice.
A. Representative Ca^{2+} transients evoked by two consecutive exposures to AMPA (5 μM, 20 s exposure) in spinal cord slices from uninflamed (left) or CFA 21 mice (right) as measured by live-cell ratiometric analysis, first in the absence and then in the presence of NTX (10 μM). B. AMPA-evoked Ca^{2+} signals were potentiated within 12 min of exposure to NTX (10 μM) in spinal cord slices from CFA 21d mice but not uninflamed mice **p<0.01 vs control response (Dunnett's post-hoc test following 2-way ANOVA.) Data represent mean ± SEM, n = 7–12 mice/group.